Phase Transitions

DOI: 10.1002/anie.201410184

Photoliquefiable Ionic Crystals: A Phase Crossover Approach for Photon Energy Storage Materials with Functional Multiplicity**

Keita Ishiba, Masa-aki Morikawa, Chie Chikara, Teppei Yamada, Katsunori Iwase, Mika Kawakita, and Nobuo Kimizuka**

Abstract: *Ionic crystals (ICs) of the azobenzene derivatives show photoinduced IC–ionic liquid (IL) phase transition (photoliquefaction) upon UV-irradiation, and the resulting cis-azobenzene ILs are reversibly photocrystallized by illumination with visible light. The photoliquefaction of ICs is accompanied by a significant increase in ionic conductivity at ambient temperature. The photoliquefaction also brings the azobenzene ICs further significance as photon energy storage materials. The cis-IL shows thermally induced crystallization to the trans-IC phase. This transition is accompanied by exothermic peaks with a total ΔH of 97.1 kJ mol^{-1}, which is almost double the conformational energy stored in cis-azobenzene chromophores. Thus, the integration of photo-responsive ILs and self-assembly pushes the limit of solar thermal batteries.*

Ionic liquids (ILs) have received increased attention because of their unique physical and chemical properties, which can be tailored based on their component chemical structures.[1,2] Along with the expanding areas of energy-related applications,[3] self-assembly[4] and interfacial phenomena[5] of ILs have pushed back new frontiers. In light of the studies on ILs in extending the bulk liquid phase to interfacial materials chemistry, the next challenge involves controlling their physical properties and functions based on the phase-transition phenomena between the ionic crystal (IC) phase and the IL phase. This phenomena is in line with the recent expectations for ILs to serve as heat storage materials.[6] Meanwhile, phase transitions between ILs and ICs usually occur below room temperature,[7] and obviously a new approach is required to control these thermodynamic phase-transition phenomena at temperatures above room temperature and to link them with distinctive functions.

To achieve the objectives, photochromism of azobenzene chromophores emerges as a prime candidate.[8] Azobenzene units have been widely employed as molecular switches because of their high quantum yields and ability to undergo reversible *trans–cis* isomerization upon sequential absorption of two different wavelengths of light.[8] The photoisomerization of azobenzenes to a high-energy metastable *cis* isomer allows storage of photon energy in the form of molecular strain energy (ca. 50 kJ mol^{-1}),[9,10] which can be released as heat in the course of the *cis–trans* thermal isomerization. These features rendered azobenzene chromophores potential candidates for the closed-cycle solar fuels, however, they have encountered the following major problems: Firstly, the exothermicity of 50 kJ mol^{-1} for *cis*-azobenzene is comparable or even smaller than the minimum gravimetric energy density desired for thermal storage materials (ca. 100 J g^{-1}).[6] Secondly, the *trans–cis* photoisomerization of azobenzene chromophores is significantly suppressed within crystals,[11] and consequently it has been studied in solutions.[9] The photoisomerization in solution inevitably results in significant decrease in the volumetric energy density.[9b] Although a hybrid solar thermal fuel using azobenzene-functionalized carbon nanotubes was reported recently,[10b] the use of nanotubes is undesirable because the presence of nanotubes not only limits the light absorbed by azobenzene chromophores but also reduces gravimetric energy density of the conjugates. Thus to date, there exists no molecular solar thermal batteries to solve these issues.

We describe herein the first example of photoresponsive ICs which show reversible photoliquefaction into ILs. This approach brings about a large increase in the energy-storage capacity. Moreover, the photoinduced IC–IL phase transition causes significant changes in ionic conductivity, thus giving multiple funtionality to the azobenzene phase-transition system. The combination of azobenzene photoisomerization and ICs–IL phase transition not only pushes the limits of current azobenzene solar thermal fuels but also provides a new perspective in designing phase crossover materials as discussed below.

Figure 1 shows chemical structures of the cationic azobenzene derivatives **1**(*n*,*m*)-X developed in this study, and they possess varied alkyl tails (*n*) and spacers methylene length (*m*), an oligo(ethylene oxide)-based ammonium group, and a counter ion (X). These compounds were designed by reference to the synthetic bilayer-forming amphiphiles.[12] Chloride, bromide, and bis(trifluoromethylsulfonyl)amide

[*] K. Ishiba, Dr. M-a. Morikawa, C. Chikara, Dr. T. Yamada, Prof. Dr. N. Kimizuka
Department of Chemistry and Biochemistry, Graduate School of Engineering, Center for Molecular Systems (CMS)
Kyushu University
744 Moto-oka Nishi-ku, Fukuoka 819-0395 (Japan)
E-mail: n-kimi@mail.cstm.kyushu-u.ac.jp
Dr. M-a. Morikawa, Prof. Dr. N. Kimizuka
JST CREST
Honcho 4-1-8, Kawaguchi, Saitama 332-0012 (Japan)
K. Iwase, M. Kawakita
DENSO CORPORATION
500-1 Minamiyama, Komenoki-cho, Nisshin, Aichi 470-0111 (Japan)

[**] This work was supported by Grant-in-Aid for Scientific Research (S) (25220805) and JST-CREST. We are grateful to Dr. Miho Ito and Mr. Yasuhiro Toyama of DENSO CORP. for stimulating discussions and technical support.

Supporting information for this article is available on the WWW under http://dx.doi.org/10.1002/anie.201410184.

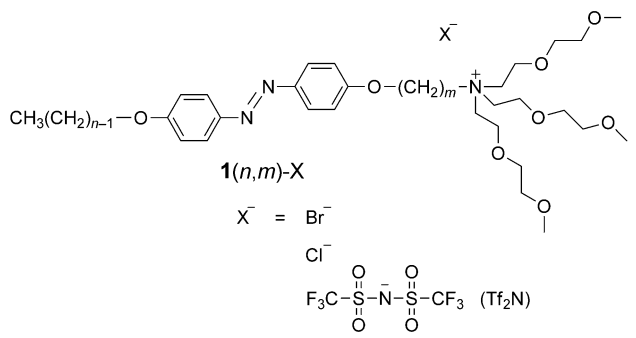

Figure 1. Chemical structure of **1**(*n*,*m*)-X.

(Tf_2N) were introduced as counterions. The oligo(ethylene oxide) units were introduced in the ammonium group with the expectation that such a flexible and bulky head group would lower the melting temperature of ICs. As expected, compounds with short alkyl chains, **1**(1,2)-Cl and **1**(1,4)-Cl, gave an IL phase at ambient temperature, thus indicating that the bulky oligoether-based ammonium group lowered the crystallinity by weakening van der Waals interactions, π–π stacking, and the Madelung energy. In contrast, the longer-alkyl chain compounds, **1**(4,6)-Br, **1**(6,4)-Cl, **1**(6,4)-Br, and **1**(8,2)-Br, were obtained in crystalline form (see Figure S1 and Table S1 in the Supporting Information). The substitution of the halide counterion for Tf_2N significantly lowered the melting point and **1**(6,4)-Tf_2N gave an IL at ambient temperature. This feature is ascribed to weakened electrostatic interactions as a result of the enhanced delocalization of anionic charge on the Tf_2N ion.[1]

Photochromic properties of the cationic azobenzene compounds were then investigated for neat ILs, ICs, and methanol solutions thereof. All these methanol solutions naturally showed reversible photoisomerization characteristics (see Figure S3). The reversible photoisomerization was also observed for the neat ILs **1**(1,2)-Cl, **1** (1,4)-Cl, and **1**(6,4)-Tf_2N, as revealed by color changes, UV/Vis spectra (for neat IL specimens), and also by ^{1}H NMR spectra obtained for $CDCl_3$ solutions. Very interestingly, the ICs **1**(6,4)-Cl, **1**(6,4)-Br, **1**(4,6)-Br, and **1**(8,2)-Br all displayed photoisomerization characteristics at ambient temperatures. Figure 2 shows the effect of photoillumination on X-ray diffraction (XRD) patterns of **1**(6,4)-Br and their polarizing optical microscopy (POM) images under crossed polarizers (inset) as a typical example. Before UV irradiation, the yellow **1**(6,4)-Br sample showed birefringence in POM images under the crossed polarizer (Figure 2a), and is consistent with the crystalline lamellar structure as observed in XRD measurements (see Figures S4–S6). After illumination of UV light by a high-pressure mercury lamp [band pass filter, $\lambda = (365 \pm 10)$ nm], the yellow crystal sample melted to give a red liquid phase within a few minutes (Figure 2b; see Movie S1). The irradiated part of the sample became dark in the POM images under the crossed polarizer, and was accompanied by an increase in n–π* absorption intensity at $\lambda = 450$ nm (see Figures S8a,b and S9a). These changes were also accompanied by disappearance of XRD patterns (Figure 2b). These observations clearly indicate that photoisomerization of

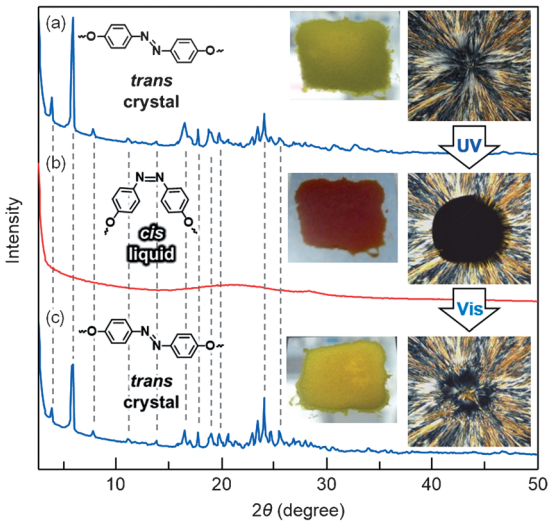

Figure 2. X-ray diffraction patterns obtained for **1**(6,4)-Br prepared on silicon wafer: a) as prepared film, b) after UV irradiation, and c) after Vis irradiation. A picture of each sample is shown as an inset. Optical microscopy images under crossed polarizers are shown in the right (substrate, glass slide). A high-pressure mercury lamp [band pass filter, $\lambda = (365 \pm 10)$ nm] was used as UV light illumination for bright-field and polarized optical microscopy. Xenon lamp (band pass filter, $\lambda = (365 \pm 10)$ nm] was used for XRD samples.

trans-**1**(6,4)-Br induced its liquefaction to the isotropic IL phase. The molar ratio of the *cis* isomer, determined by ^{1}H NMR spectroscopy (in $CDCl_3$), was about 80%. Meanwhile, upon illumination of the visible light [$\lambda = (470 \pm 20)$ nm] to the photoliquefied ILs, crystallization occurred reversibly within 1 minute (Figure 2c; see Movie S1), and was accompanied by a decrease in the n–π* absorption intensity of *cis* isomer at $\lambda = 450$ nm (see Figure S8c,d) and reappearance of the XRD patterns characteristic to the *trans*-azobenzene compound (Figure 2c). The reversible photoliquefaction and photocrystallization were similarly observed for the ICs of **1**(6,4)-Cl, **1**(4,6)-Br, and **1**(8,2)-Br at room temperature (see Figures S10–12). Thus, these ICs show totally reversible photoliquefaction and photocrystallization phenomena which are superior features surpassing the previously reported solid–liquid phototransition systems.[13]

The photon energy storage capacity of the present photo-induced IC–IL phase-transition system was then investigated for **1**(6,4)-Br. The ionic liquid **1**(6,4)-Tf_2N was taken as a reference to determine the photon energy converted and stored in the IL phase. These samples were photoisomerized in advance and stored in the *cis* form. Figures 3 a and b shows DSC thermograms obtained for ILs of *cis*-**1**(6,4)-Tf_2N and *cis*-**1**(6,4)-Br, respectively. Upon heating *cis*-**1**(6,4)-Tf_2N, a broad exothermic peak was observed around at 49 °C with a ΔH value of 46.1 kJ mol^{-1}, which corresponds to the ΔH value of 51.8 kJ mol^{-1} for the pure *cis* isomer (Figure 3a). This peak is associated with the thermally induced *cis–trans* isomerization of the IL, and the observed change in enthalpy (ΔH) is consistent with the reported energy ($\Delta H_{cis-trans}$) stored in a *cis*-azobenzene chromophore.[10a] In contrast, when the photoliquefied *cis*-**1**(6,4)-Br was heated, two exothermic

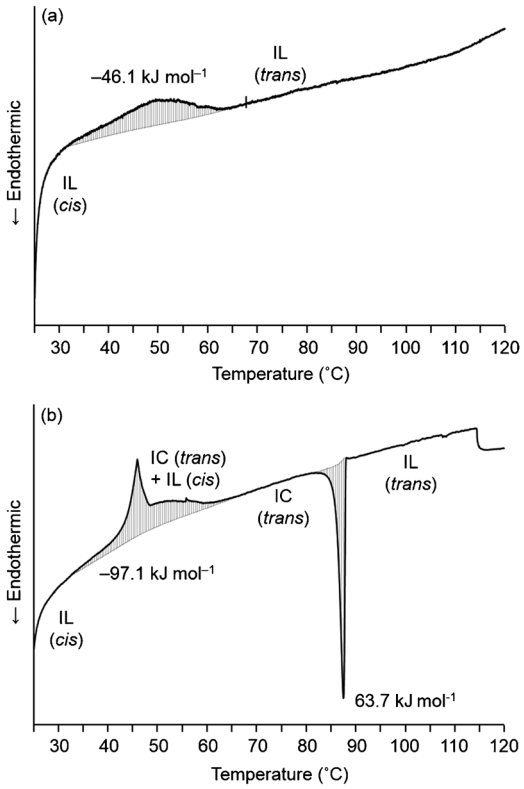

Figure 3. DSC thermograms of *cis*-azobenzene derivatives: a) *cis*-**1**(6,4)-Tf_2N (IL) and b) *cis*-**1**(6,4)-Br. Each sample contained the *cis*-form in 89 mol% as determined by ^{1}H NMR sprctroscopy in $CDCl_3$. Heating rate, 0.2 °C min^{-1}. The exothermic peaks are affected by the heating rate, as shown in Figure S13.

peaks were found to coexist (Figure 3b). In addition to the broad exothermic peak associated with the thermal *cis–trans* isomerization (temperature range: 34–65 °C), a sharp exothermic peak is observed around at 46 °C. This peak is ascribed to the crystallization of *trans*-**1**(6,4)-Br formed by thermally induced isomerization of *cis*-**1**(6,4)-Br IL, as discussed later. The total ΔH determined for the sharp and broad exothermic peaks observed in Figure 3b amounts to 97.1 kJ mol^{-1}, which is almost double the energy stored in a *cis*-azobenzene chromophore. It goes over the necessary standards for the specific energy required for thermophysical storages (the specific energy requirement of 100 J g^{-1} corresponds to 75.7 kJ mol^{-1} for **1**(6,4)-Br).[6] Meanwhile, further heating of the sample gave a sharp endothermic peak at 87 °C (ΔH, 63.7 kJ mol^{-1}) which is due to the melting of IC (*trans*-**1**(6,4)-Br) phase.

The unique thermal properties observed for the *cis*-**1**(6,4)-Tf_2N and *cis*-**1**(6,4)-Br ILs were then scrutinized by performing optical microscopy observation concurrently with the DSC measurement. Upon heating, the IL of *cis*-**1**(6,4)-Tf_2N showed a red–yellow color change, thus reflecting the thermal *cis–trans* isomerization in the IL phase (Figure 4a; see Movie S2). Meanwhile, heating of the photoliquefied *cis*-**1**(6,4)-Br IL showed growth of a crystalline phase at around at 35 °C and it was clearly visible as the red–dark red color change (Figure 4b; see Movie S3 and Figure S14). This color change is consistent with the crystallization of *trans*-**1**(6,4)-Br in the *cis*-**1**(6,4) IL phase. The dark red color of the mixed state of IC and IL then turned ocher at around at 60 °C, thus indicating the completion of thermal isomerization. These thermally induced IL–IC phase-transition characteristics are consistent with the time dependence of XRD patterns observed for *cis*-**1**(6,4)-Br (see Figure S15). The melting of the ocher crystalline *trans*-**1**(6,4)-Br into the yellow IL phase was further observed by continuous heating of the specimen to 87 °C, as expected from the DSC thermogram (Figure 3b; see Figure S14d).

The photoisomerization of ionic crystals shows multiple fuctionality, as well as reversible liquefaction phenomena and changes in optical properties. As an example, we performed alternating current (AC) impedance measurements for **1**(6,4)-Br and **1**(6,4)-Tf_2N to examine the effect of photoinduced phase transition on ionic conductivity (see Figures S16–18). In Figure 5a, the *trans*-**1**(6,4)-Tf_2N IL gave ionic conductivity of 2.0×10^{-5} S cm^{-1} (open circle), which is about two orders of magnitude lower than that of the typical ionic liquid 1-methyl-4-butyl imidazolium Tf_2N,[14] thus reflecting larger viscosity of the azobenzene IL. Upon *trans–cis* photoisomerization of **1**(6,4)-Tf_2N IL by illumination with UV light [$\lambda = (365 \pm 10)$ nm], the ionic conductivity showed a slight increase to 2.1×10^{-5} S cm^{-1} (filled circle). Additional illumination of the *cis*-**1**(6,4)-Tf_2N IL with visible light [$\lambda = (480 \pm 10)$ nm] caused reversible decrease to the original value, and these changes are reversible with respect to the alternative illumination by UV and visible light (Figure 5a; see Figure S18a). To date, photoinduced changes in the ionic conductivity of azobenzene derivatives have been measured in solutions.[15c,16] The present data clearly indicate that *trans–cis* isomerization of **1**(6,4)-Tf_2N IL caused increase in the ion mobility in consequences of the changes in molecular shape and intermolecular interactions.[17]

Meanwhile, the *trans*-**1**(6,4)-Br in the IC phase showed a considerably lower ionic conductivity of 4.2×10^{-10} S cm^{-1},

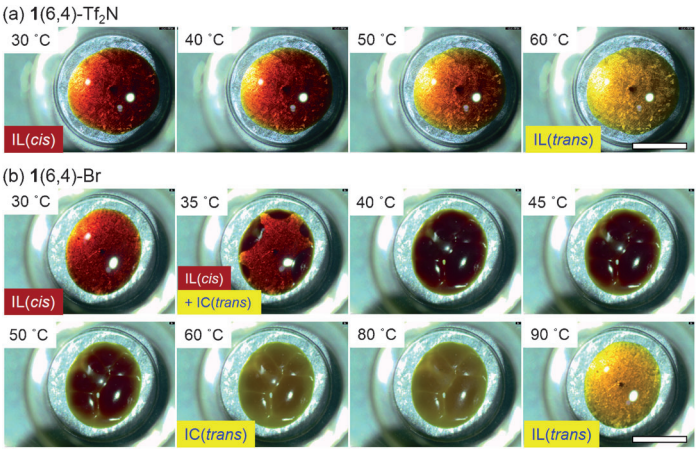

Figure 4. Pictures of ILs in the course of DSC measurement. a) **1**(6,4)-Tf_2N and b) **1**(6,4)-Br. The specimens were photoliquefied prior to the DSC measurements. DSC measurements were conducted without sealing the aluminum crucibles (heating rate, 0.2 °C min^{-1}). Scale bar: 3 mm.

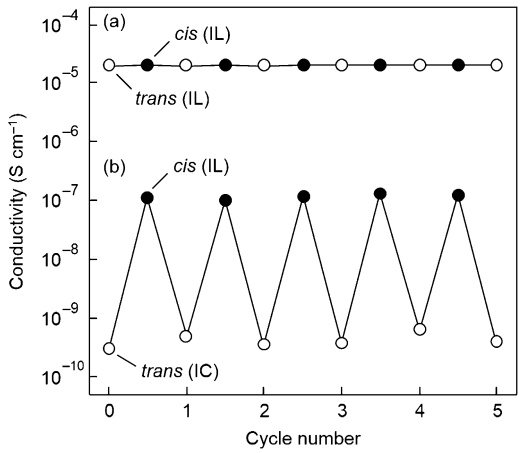

Figure 5. Changes in ionic conductivity upon repeated UV and Vis irradiation for a) **1**(6,4)-Tf_2N and b) **1**(6,4)-Br. UV-irradiation of the *trans*-azobenzene compounds (open circle) give *cis*-azobenzene compounds (filled circles) and the changes are reversible.

thus reflecting suppressed migration of ionic species in the crystalline state (Figure 5b). Very interestingly, upon photoliquefaction of *trans*-**1**(6,4)-Br, a salient increase in ionic conductivity was observed to be 1.2×10^{-7} S cm^{-1}, which is 280 times higher than that of the *trans*-**1**(6,4)-Br ionic crystal. The observed remarkable change in ionic conductivity is reasonably explained by the enhanced mobility of ionic species in the *cis*-IL. The change in ionic conductivity also showed good reversibility upon repeated illumination of the Vis and UV light (Figure 5b), thus reflecting the totally reversible IC–IL phase transition. Thus, the reversible photoliquefaction of ICs leads to concomitant control on ionic conductivity at ambient temperature. The lower ionic conductivity observed for *cis*-**1**(6,4)-Br IL, compared to that of *cis*-**1**(6,4)-Tf_2N, is ascribed to the lower self-diffusion coefficient of the bromide ion, as reported for the other ionic liquids.[18,19] The changes in ionic conductivity exceeding two orders of magnitude at room temperature are overwhelming those reported for liquid crystalline systems which require high operating temperatures (usually above 100 °C) and laborious sample treatments.[20]

In conclusion, ICs formed by azobenzene derivatives showed photoliquefaction into ILs. The photoliquefaction approach significantly enhances the photon energy storage capacity of azobenzene chromophores. Furthermore, ionic conductivity was prominently increased concurrently with the photoliquefaction. To the best of our knowledge, this is the first example of reversible photoliquefaction and crystallization of ICs. Although photoisomerizable ILs have been recently reported,[15] none of them show the IC–IL phase transition. The photoisomerization of azobenzene chromophores in the condensed phase has been largely limitted to thin crystalline needles,[21] liquid crystals,[20] liquid crystalline polymers.[22] Recently, nonionic azobenzene derivatives of macrocyclic azobenzenophane,[13] carbohydrate conjugates,[23] and oligoether-appended azobenzene compounds[24] were shown to display photoinduced solid–liquid phase-transition phenomena, however their photon energy storage properties have not been the subject of research.[13,15,20–24] The integration of self-assembly and photoinduced IC–IL transition dissolve limitations in the current solar thermal storage technology and provides a design principle for developing multifunctional ILs. It would provide a new perspective in the study of condensed soft materials which could be referred to as phase crossover chemistry.

Received: October 17, 2014
Published online: December 5, 2014

Keywords: energy storage · ionic liquids · phase transitions · photochemistry · self-assembly

[1] a) H. Ohno, *Electrochemical Aspects of Ionic Liquids*, 2nd ed., Wiley, Hoboken, **2011**; b) H. Niedermeyer, J. P. Hallett, I. J. Villar-Garcia, P. A. Hunt, T. Welton, *Chem. Soc. Rev.* **2012**, *41*, 7780 – 7802.
[2] a) R. Giernoth, *Angew. Chem. Int. Ed.* **2010**, *49*, 2834 – 2839; *Angew. Chem.* **2010**, *122*, 2896 – 2901; b) J. H. Davis, Jr., *Chem. Lett.* **2004**, *33*, 1072 – 1077.
[3] D. R. MacFarlane, N. Tachikawa, M. Forsyth, J. M. Pringle, P. C. Howlett, G. D. Elliott, J. H. Davis, Jr., M. Watanabe, P. Simon, C. A. Angell, *Energy Environ. Sci.* **2014**, *7*, 232 – 250.
[4] a) N. Kimizuka, T. Nakashima, *Langmuir* **2001**, *17*, 6759 – 6761; b) T. Nakashima, N. Kimizuka, *Langmuir* **2011**, *27*, 1281 – 1285; c) T. Nakashima, N. Kimizuka, *Polym. J.* **2012**, *44*, 665 – 671; d) T. L. Greaves, C. J. Drummond, *Chem. Soc. Rev.* **2013**, *42*, 1096 – 1120.
[5] a) T. Nakashima, N. Kimizuka, *J. Am. Chem. Soc.* **2003**, *125*, 6386 – 6387; b) M.-a. Morikawa, A. Takano, S. Tao, N. Kimizuka, *Biomacromolecules* **2012**, *13*, 4075 – 4080; c) T. Torimoto, T. Tsuda, K.-i. Okazaki, S. Kuwabata, *Adv. Mater.* **2010**, *22*, 1196 – 1221.
[6] I. Gur, K. Sawyer, R. Prasher, *Science* **2012**, *335*, 1454 – 1455.
[7] T. Endo, T. Kato, K. Tozaki, K. Nishikawa, *J. Phys. Chem. B* **2010**, *114*, 407 – 411.
[8] a) H. M. D. Bandara, S. C. Burdette, *Chem. Soc. Rev.* **2012**, *41*, 1809 – 1825; b) D. Bléger, Z. Yu, S. Hecht, *Chem. Commun.* **2011**, *47*, 12260 – 12266.
[9] a) T. J. Kucharski, Y. Tian, S. Akbulatov, R. Boulatov, *Energy Environ. Sci.* **2011**, *4*, 4449 – 4472; b) J. Olmsted, J. Lawrence, G. G. Yee, *Solar Energy.* **1983**, *30*, 271 – 274.
[10] a) A. M. Kolpak, J. C. Grossman, *Nano Lett.* **2011**, *11*, 3156 – 3162; b) T. J. Kucharski, N. Ferralis, A. M. Kolpak, J. O. Zheng, D. G. Nocera, J. C. Grossman, *Nat. Chem.* **2014**, *6*, 441 – 447.
[11] M. Irie, *Bull. Chem. Soc. Jpn.* **2008**, *81*, 917 – 926.
[12] M. Shimomura, R. Ando, T. Kunitake, *Ber. Bunsenges. Phys. Chem.* **1983**, *87*, 1134 – 1143.
[13] a) Y. Norikane, Y. Hirai, M. Yoshida, *Chem. Commun.* **2011**, *47*, 1770 – 1772; b) E. Uchida, K. Sakaki, Y. Nakamura, R. Azumi, Y. Hirai, H. Akiyama, M. Yoshida, Y. Norikane, *Chem. Eur. J.* **2013**, *19*, 17391 – 17397; c) M. Hoshino, E. Uchida, Y. Norikane, R. Azumi, S. Nozawa, A. Tomita, T. Sato, S. Adachi, S. Koshihara, *J. Am. Chem. Soc.* **2014**, *136*, 9158 – 9164.
[14] M. Galiński, A. Lewandowski, I. Stępniak, *Electrochim. Acta* **2006**, *51*, 5567 – 5580.
[15] a) L. C. Branco, F. Pina, *Chem. Commun.* **2009**, 6204 – 6206; b) A. Kawai, D. Kawamori, T. Monji, T. Asaka, N. Akai, K. Shibuya, *Chem. Lett.* **2010**, *39*, 230 – 231; c) S. Zhang, S. Liu, Q. Zhang, Y. Deng, *Chem. Commun.* **2011**, *47*, 6641 – 6643.
[16] T.-T.-T. Nguyen, D. Türp, M. Wagner, K. Müllen, *Angew. Chem. Int. Ed.* **2013**, *52*, 669 – 673; *Angew. Chem.* **2013**, *125*, 697 – 701.
[17] S. Tsuzuki, *ChemPhysChem* **2012**, *13*, 1664 – 1670.
[18] M. Yoshizawa, H. Ohno, *Electrochim. Acta* **2001**, *46*, 1723 – 1728.

[19] B.-K. Cho, *RSC Adv.* **2014**, *4*, 395 – 405.
[20] B. Soberats, E. Uchida, M. Yoshio, J. Kagimoto, H. Ohno, T. Kato, *J. Am. Chem. Soc.* **2014**, *136*, 9552 – 9555.
[21] H. Koshima, N. Ojima, H. Uchimoto, *J. Am. Chem. Soc.* **2009**, *131*, 6890 – 6891.
[22] a) T. Ikeda, O. Tsutsumi, *Science* **1995**, *268*, 1873 – 1875; b) N. Hosono, T. Kajitani, T. Fukushima, K. Ito, S. Sasaki, M. Takata, T. Aida, *Science* **2010**, *330*, 808 – 811.
[23] H. Akiyama, M. Yoshida, *Adv. Mater.* **2012**, *24*, 2353 – 2356.
[24] Y. Okui, M. Han, *Chem. Commun.* **2012**, *48*, 11763 – 11765.

